ACS APPLIED MATERIALS & INTERFACES

Research Article

www.acsami.org

Microfluidic Assay To Study the Combinatorial Impact of Substrate Properties on Mesenchymal Stem Cell Migration

Nishanth V. Menon,[†] Yon Jin Chuah,[†] Samantha Phey,[‡] Ying Zhang,[†] Yingnan Wu,[†] Vincent Chan,[†] and Yuejun Kang*[,†]

[†]School of Chemical and Biomedical Engineering, Nanyang Technological University, 62 Nanyang Drive, Singapore 637459

[‡]Hwa Chong Institution, 661 Bukit Timah Road, Singapore 269734

Supporting Information

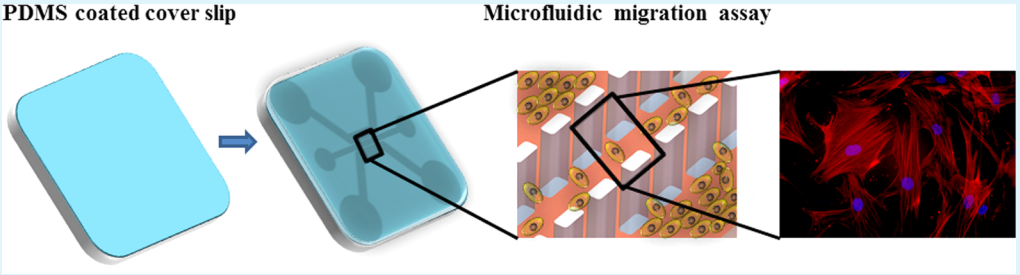

ABSTRACT: As an alternative to complex and costly in vivo models, microfluidic in vitro models are being widely used to study various physiological phenomena. It is of particular interest to study cell migration in a controlled microenvironment because of its vital role in a large number of physiological processes, such as wound healing, disease progression, and tissue regeneration. Cell migration has been shown to be affected by variations in the biochemical and physical properties of the extracellular matrix (ECM). To study the combinatorial impact of the ECM physical properties on cell migration, we have developed a microfluidic assay to induce migration of human bone marrow derived mesenchymal stem cells (hBMSCs) on polydimethylsiloxane (PDMS) substrates with varying combinatorial properties (hydrophobicity, stiffness, and roughness). The results show that although the initial cell adhesion and viability appear similar on all PDMS samples, the cell spreading and migration are enhanced on PDMS samples exhibiting intermediate levels of hydrophobicity, stiffness, and roughness. This study suggests that there is a particular range of substrate properties for optimal cell spreading and migration. The influence of substrate properties on hBMSC migration can help understand the physical cues that affect cell migration, which may facilitate the development of optimized engineered scaffolds with desired properties for tissue regeneration applications.

KEYWORDS: *human-bone-marrow-derived mesenchymal stem cells, extracellular matrix, cell migration and spreading, substratum properties, roughness, stiffness, wettability*

INTRODUCTION

Tissue engineering is an integral part of regenerative medicine, which involves the repair and regeneration of impaired tissues or organs due to an injury or a disease. Stem cell mediated tissue regeneration, especially for bone and cartilage repair,[1−3] has been extensively studied in the past decade due to its multipotent therapeutic capability. The stem cells are usually introduced either as cell suspensions[4] or are homed in biodegradable scaffolds and implanted at the site of injury.[3,5] For the latter technique, the scaffolds are critical because they significantly influence the formation of extracellular matrix (ECM) of the regenerated tissues. The effects of ECM on cell behaviors, such as viability, spreading, migration, intercellular communication and differentiation, have been discussed extensively in the literature.[6−8]

Among these cell behaviors, cell migration is of particular interest and plays a vital role in many important physiological processes, such as embryogenesis, disease progression, wound healing and tissue regeneration.[9] The ECM comprises cell-secreted proteins and other biomolecules, providing physical and chemical frameworks and cues to the surrounding cells. The physical cues are induced by the inherent physical properties of the scaffolds, including topography, stiffness, hydrophobicity, as well as other properties exhibited at the cell-scaffold interface. The chemical cues involve the biomolecular composition of the ECM, such as surface-bound ligands, adherent proteins and chemoattractant gradient, which activate the biochemical receptors on the cell membrane and direct their locomotion. Although these complex biophysical and biochemical cues usually work in coordination to guide cell migration and tissue development,[9,10] recent advances in micro- and nanotechnologies have made it possible to explore the effects solely due to a single or multiple physical cues.[11−13] In scaffold-based tissue regeneration using stem cells, it is

Received: April 30, 2015
Accepted: July 17, 2015
Published: July 17, 2015

DOI: 10.1021/acsami.5b03753
ACS Appl. Mater. Interfaces 2015, 7, 17095−17103

important for the cells to migrate toward the site of injury, proliferate and differentiate into the desired tissues. Considering the potential toxicity of introducing artificial biochemical factors, it becomes particularly attractive to induce and modulate cell migration by controlling the physical or mechanical properties of biocompatible scaffold to achieve effective therapeutics.[14,15]

Conventionally, cell migration was studied using scratch assay[16] or Boyden's chamber.[17] Recently, microfluidics-based lab-on-a-chip technology has found extensive applications in many exploratory cell research in vitro.[18,19] The major advantages of lab-on-a-chip devices over conventional cell-based assays include significantly reduced sample and reagent consumption, high sensitivity, and rapid speed of assay. Some microfluidic devices are able to precisely control fluid flow and generate chemical gradient in microscale,[20,21] which is extremely difficult in conventional migration assays such as Boyden's chamber. A large variety of microfluidic in vitro models have been created and proved to be much more advantageous than conventional in vitro models.[22] Polydimethylsiloxane (PDMS) is a common molding material for fabricating high-resolution micro- and nanostructures in lab-on-a-chip devices owing to its chemical inertness, biocompatibility,[23] permeability to gases,[24] and optical transparency. Moreover, the surface properties of PDMS, such as stiffness, roughness and hydrophobicity, can be easily tuned by adjusting the mixing ratio of the prepolymer to the cross-linker. These features have made PDMS a capable tool to study the impact of different substrate physical properties on cell behaviors.[25−27]

Previously, the individual effects of surface property on cell migration have been studied extensively. It was shown that hydrophobic surfaces (contact angle = 98.5° ± 2.3°) improved endothelial cell migration as compared to hydrophilic surfaces (contact angle <90°).[28] Moreover, the collective migration of HuH7 cancer cells was favored on a PDMS surface with root-mean-square (RMS) roughness of 2 nm as compared to those with RMS roughness of 60 nm.[12] Additionally, NIH 3T3 cells were observed to migrate from a softer surface toward a stiffer surface owing to the lower cell traction force required on the softer substrate, which also resulted in a faster migration rate on the softer substrates.[29] More relevant studies reported similar phenomenon that the collective migration of fibroblast and epithelial cells was promoted on substrates with lower rigidity, suggesting the weaker integrin-cytoskeleton linkages[10] and hence dynamic cell adhesion on less rigid surfaces.[30] Further studies indicated that, for a specific surface ligand density, there existed an optimal substrate rigidity at which cell migration reached maximum level.[31−34] As shown in these early investigations, variation of a single aspect of surface properties could affect cell migration profoundly. On the other hand, for many common materials, the alteration of one particular substrate property may cause the change of others. For example, the stiffness of PDMS substrate can be changed by adjusting the mixing ratio of prepolymer base to the cross-linker,[35] which also alters the surface roughness as well as hydrophobicity. However, these multiple aspects of substratum properties, including hydrophobicity, roughness and stiffness, and their combinatorial influence on cell migration remain to be elucidated.

In this work, we aim to understand the combinatorial impact of PDMS substrate properties on the migration of human bone marrow derived mesenchymal stem cells (hBMSCs), which are a major type of stem cells that have important applications in tissue engineering and regenerative medicine. BMSCs are featured by their multipotency to differentiate into osteogenic, chondrogenic, and adipogenic lineages for tissue and bone regeneration.[1−3] BMSCs can also be easily acquired from many mesenchymal origins available from human and other mammals. Therefore, BMSCs have become a popular cell type to explore the emerging stem-cell based therapeutics. Many researchers have also used BMSCs to culture organ-on-a-chip as in vitro models to study various physiological phenomena.[36] hBMSC migration is a vital process during scaffold-based stem cell therapy, where the homing cells from the scaffold migrate toward the damaged tissue and eventually differentiate into specific tissues.[3] It is important to understand the optimal physical cues that would allow for improved hBMSC migration to optimize the therapeutic effect. In this proof-of-concept study, a microfluidic migration assay is developed using different PDMS substrates formulated with various levels of cross-linking. Cell adhesion and proliferation are first measured to characterize the biocompatibility of the substrate, following which the cell spreading and migration in the microfluidic chip are compared to elucidate the combinatorial impact of the substratum physical properties.

MATERIALS AND METHODS

Microfluidic Chip Preparation. A 3-compartment microfluidic chip was designed comprising a central channel of 500 μm in width and two side-channels of 800 μm in width (Figure 1). The three compartments were separated from each other by rectangular pillar (200 μm × 100 μm) arrays to control the liquid flow in specific compartments and thus allow for selective cell seeding on the chip. The chip was fabricated following soft lithography method.[37] In brief, a layer of negative photoresist SU8−2050 (MicroChem, MA, USA) was spin-coated on a silicon wafer followed by soft baking at 95 °C for 45 min and exposure to UV radiation (365 nm) through a photomask. The wafer was baked again at 95 °C for 15 min before being developed in SU8 developer (MicroChem, MA, USA). The thickness of the mold was measured as 170 μm. PDMS prepolymer mixed with curing agent at ratio of 10:1 by weight (Sylgard 184, Dow Corning, MI, USA) was cast on the SU8 mold, followed by degassing and curing at 70 °C for 3 h. The inlets of the chip were created by punching holes in the PDMS slab. PDMS of different base to curing agent ratio (5:1, 10:1, 20:1, and 40:1) were spin-coated on glass coverslips (22 mm × 22 mm) and cured at 70 °C for 3 h to create the substrates with different physical properties. The surfaces of the PDMS chips and substrates were activated using a plasma cleaner (Harrick Plasma, NY, USA) before they were bonded together. The sealed chip was further processed for cell culture following the procedures as described previously.[38] Briefly, all three compartments inside the chip were coated with 20 μg/mL fibronectin for 1 h at 37 °C, followed by washing with 1× PBS and drying at 40 °C for 24 h. A second layer of fibronectin was coated on two side-compartments only to enhance cell attachment and proliferation.

Surface Characterization. The surface roughness, stiffness and hydrophobicity of the PDMS substrates coated with fibronectin were characterized using the following methods. An optical tensiometer (Attension Theta, Sweden) was used to measure the surface hydrophobicity by characterizing the water contact angle. Five microliters of milli-Q water was dropped on the sample surface and the profile of the water droplet was captured using a high resolution camera. The contact angle was calculated by the drop shape analysis software using the static sessile drop tangent method.

The surface roughness and stiffness of the PDMS substrates were determined by atomic force microscopy (AFM, MFP-3D, Asylum Research, CA, USA). The AFM probe with a silicon tip (radius 28 ± 10 nm and spring constant 0.5−4.4 N/m) was used and the measurements were performed in tapping mode. 20 μm × 20 μm topographical images with resolution of 256 pixels were scanned at 0.8

DOI: 10.1021/acsami.5b03753
ACS Appl. Mater. Interfaces 2015, 7, 17095−17103

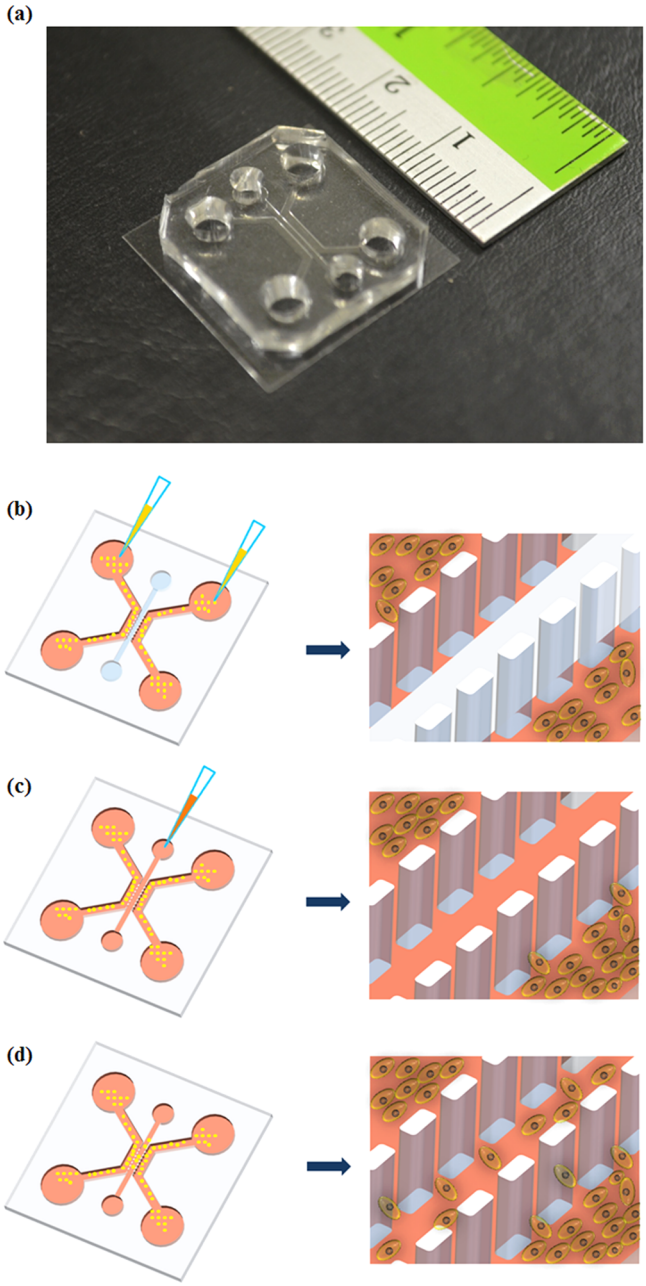

Figure 1. (a) Microfluidic chip design and size. (b) Schematic of cell seeding from the side compartments. (c) 24 h after cell seeding, cell culture medium was introduced into the central channel connecting both side-compartments. (d) Cell migration into the central compartment during subsequent culture.

Hz using a set point of 0.7 V. The probe used for stiffness measurement was a modified silicon nitride AFM cantilever (NovaScan, USA) (spring constant 0.01 N/m) with a polystyrene spherical tip (4.5 μm in diameter). The details for the stiffness measurement (elastic modulus) can be found in a previous report.[39]

Mesenchymal Stem Cell Culture and Seeding. hBMSCs were expanded using Dulbecco's modified eagle medium (DMEM) supplemented with 10% fetal bovine serum (FBS) and 1% Penicillin-streptomycin in a culture flask at 37 °C in an incubator with humidified atmosphere and 5% CO_2. Once the cells reached 80% confluence, they were resuspended using 0.25% EDTA-trypsin at density of 10^6 cells per ml. Approximately 60 μL of cell suspension was introduced into the side-compartments of the microfluidic chip (Figure 1b). The culture medium was changed every 24 h to replenish nutrients on the chip. The cell culture was maintained in a static environment throughout the experiment. All the culture reagents were purchased from Life Technologies, Singapore.

Cell Adhesion and Proliferation. To determine the adhesion and proliferation of the hBMSCs on different substrates, PDMS prepared with different prepolymer to curing agent ratios were placed on 4-well plates and coated with fibronectin. Cyquant cell proliferation assay (Life Technologies, Singapore) was used to quantify the relative cell adhesion across different fibronectin-coated PDMS substrates. Approximately, 1×10^4 cells/cm^2 were seeded onto the PDMS substrates and cultured for 60 min at 37 °C in a humidified CO_2 incubator. The cells were washed with 1× PBS twice and then frozen at −80 °C overnight. The samples were thawed and incubated with cell lysis buffer containing CyQUANTGR dye as per the manufacturer's instructions. The fluorescence was measured at excitation of 485 nm and emission of 535 nm using a microplate reader (Infinite M200 series, Tecan Asia, Singapore).

The cell proliferation was measured over 7 days using Prestoblue cell viability assay. Briefly, 1×10^4 hBMSCs were seeded onto different fibronectin-coated PDMS substrates. After 24 h, the cells were washed and incubated with 10% Prestoblue reagent supplemented in DMEM for 1 h. The cell viability was calculated based on the absorbance measured at 570 and 600 nm using a microplate reader (Infinite M200 Pro, Tecan Asia, Singapore). The assay was repeated every alternate day. All the reagents were acquired from Life Technologies, Singapore.

Cell Spreading and Migration. To investigate the influence of substratum properties on cell spreading and migration, hBMSCs were cultured and monitored in microfluidic chips sealed onto coverslips that were precoated with PDMS of different cross-linking levels. The cells were initially cultured in two side-compartments in this 3-chamber microfluidic chip, while the central compartment was empty without any culture medium (Figure 1b). After overnight culture, medium was introduced to the central compartment hence connecting both side-compartments (Figure 1c) and allowing for the cells to migrate into the center of the chip (Figure 1d and Figure S1 in Supporting Information). At the end of day 7, the cells were stained with DAPI (for nucleus) and TRITC-conjugated phalloidin (for F-actin cytoskeleton). The cytoskeleton staining allowed for measuring the spreading area of individual cells. The collective cell migration was quantified by two methods: the nucleus staining enabled cell number counting in the central channel, while the cytoskeleton staining could help measure the entire area covered by all migrating cells in the central compartment. Briefly, the cells were fixed with 10% formalin (Sigma-Aldrich, Singapore) overnight, followed by washing with 1× PBS thrice and staining with TRITC-conjugated phalloidin and DAPI as per the manufacturer's instructions. Both dyes were purchased from Life Technologies, Singapore. The cell images were taken using a fluorescence microscope (IX71, Olympus, Singapore). The areas covered by individual cells and cell population in the central compartment were analyzed using Image-Pro Plus (Media Cybernetics, Rockville, MD, USA).

Surface Protein Density. The density of fibronectin coated on the PDMS substrates was determined using micro-BCA protein assay (Thermo Scientific, Singapore). All PDMS substrates were coated with 20 μg/mL fibronectin for 1 h at 37 °C. The samples were then washed thrice with 1× PBS and placed in a drying oven at 40 °C for 24 h. The substrate protein density was then measured at 562 nm using a microplate reader (Infinite M200 Pro, Tecan Asia, Singapore).

Quantitative Real Time Polymerase Chain Reaction (qRT PCR). To understand the effects of different PDMS substrates on hBMSC migration, the gene expressions of cellular adhesion proteins that may influence cell migration, including paxillin and N-cadherin,[40,41] were quantified using qRT-PCR (StepOne Plus, Life Technologies, Singapore). Briefly, cells were seeded in 4-well plates containing different PDMS substrates precoated with fibronectin. After 5 days of culture, the total cellular RNA was extracted using RNeasy Mini Kit 250 (Qiagen, Singapore). Approximately, 100 ng of RNA of each sample was reverse-transcribed into complementary DNA (cDNA) using iScript Reverse Transcriptase Supermix (Bio-Rad, Singapore). Quantitative real-time PCR assays of the target genes were

DOI: 10.1021/acsami.5b03753
ACS Appl. Mater. Interfaces 2015, 7, 17095−17103

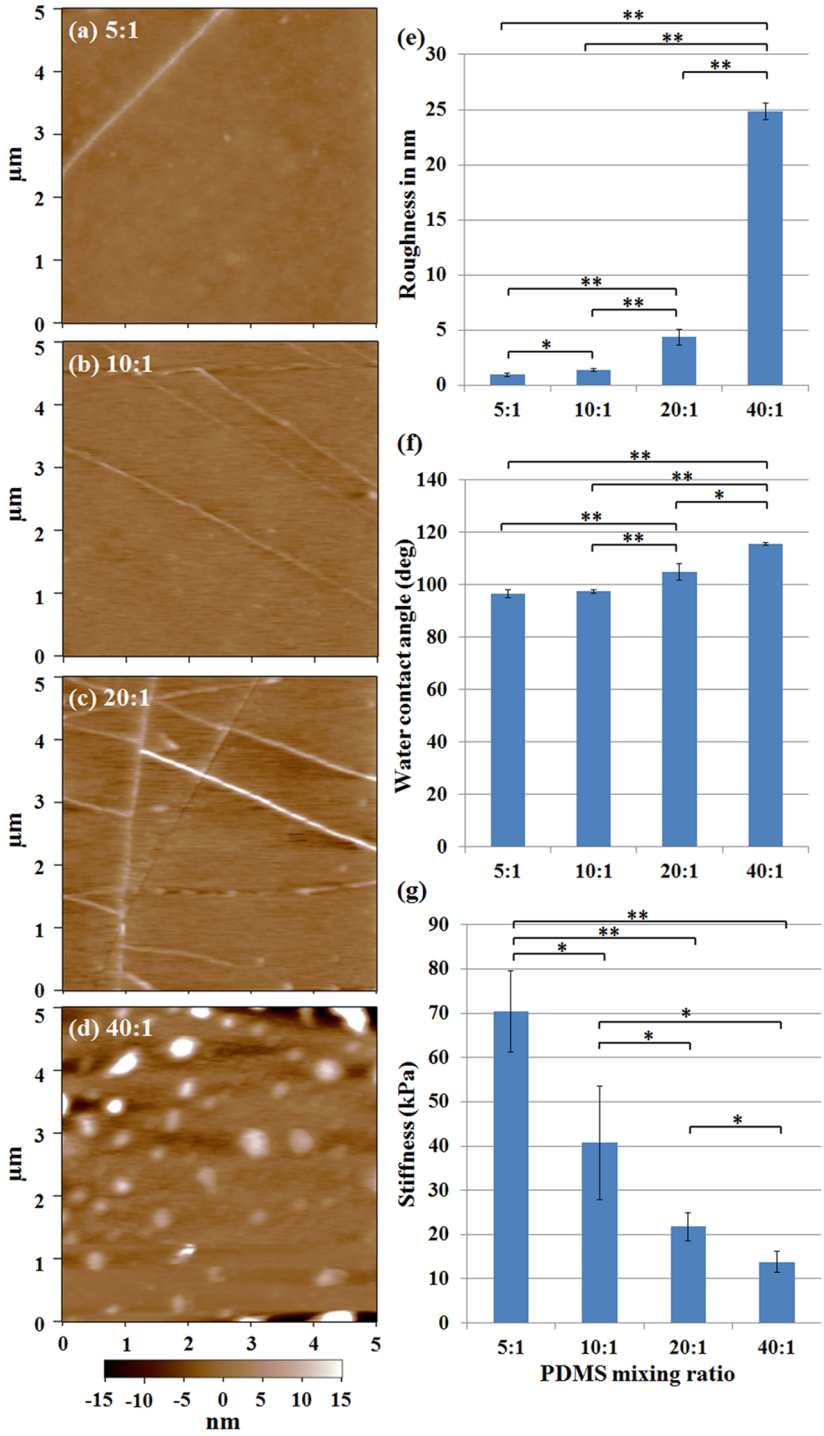

Figure 2. Characterization of the surface properties of fibronectin-coated PDMS. (a–d) AFM images of the PDMS substrates made with mixing ratio of 5:1, 10:1, 20:1, and 40:1, respectively. (e) RMS roughness (**p < 0.0001, *p < 0.05, n = 5). (f) Water contact angle (**p < 0.0001, *p < 0.05, n = 4). (g) Surface stiffness (**p < 0.0001, *p < 0.05, n = 3).

performed using StepOne Plus on a 96-well optical reaction plate (Bio-Rad, USA). Each well contained a mixture of 10 μL of Power SYBR green PCR master mix (Life Technologies, Singapore), 0.24 μL forward primer and reverse primer, and 10 μL of reverse transcribed cDNA. The sequence of the primers is listed in Table S1 (Supporting Information). All primers were purchased from IDT, Singapore. The gene expression were normalized to GADPH mRNA level in the corresponding samples and then to the expression level of the targeted gene on PDMS substrate with mixing ratio of 5:1.

Statistical Analysis. Student's t test was used for statistical analysis of all experimental results. A p-value of less than 0.05 ($p^* < 0.05$, $n \geq 3$) was considered to be statistically significant.

RESULTS AND DISCUSSION

In this study, four different mixing ratios (5:1, 10:1, 20:1, and 40:1) of PDMS was used to change the level of cross-linking and hence the surface properties. The AFM characterization illustrated the surface topography (Figure 2a–d) of the PDMS substrates and the RMS roughness increased as the mixing ratio

DOI: 10.1021/acsami.5b03753
ACS Appl. Mater. Interfaces 2015, 7, 17095–17103

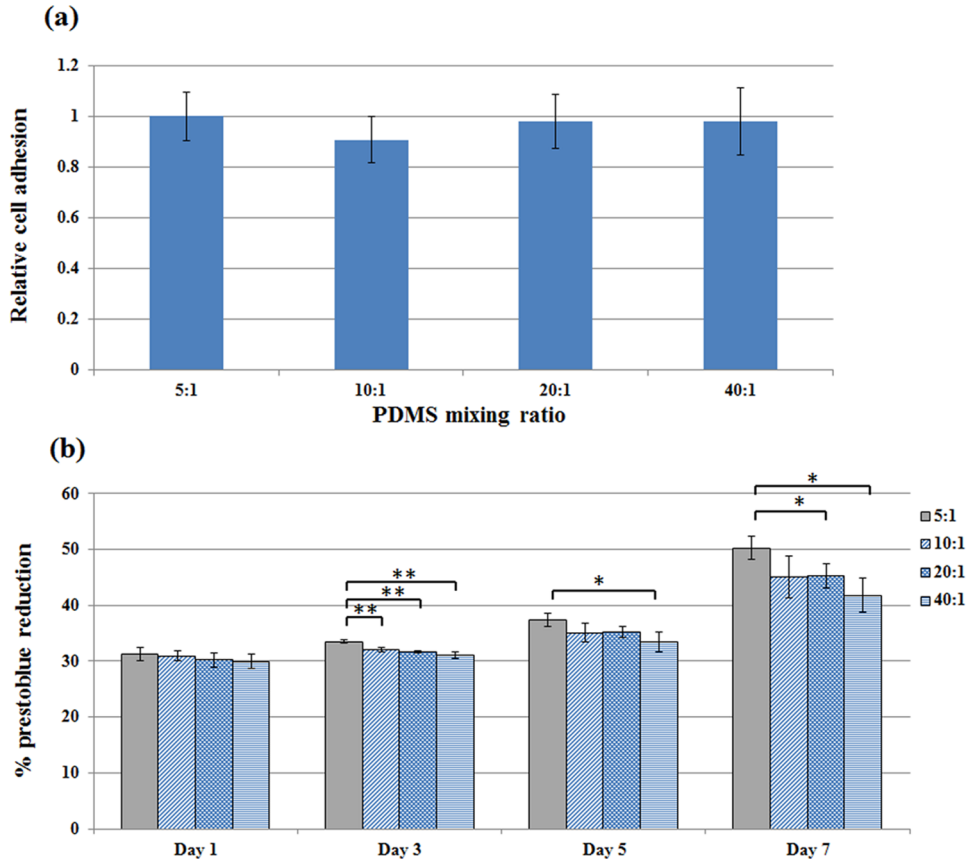

Figure 3. (a) Cell adhesion at 1 h after seeding normalized against the data on 5:1 PDMS. (b) Cell viability assays over 7 days on different PDMS substrates. $^{**}p < 0.0001$, $^{*}p < 0.05$, $n = 3$.

changed from 5:1 (0.96 ± 0.17 nm) to 40:1 (24.83 ± 0.76 nm) (Figure 2e). The highest proportion of curing agent (5:1) rendered the smoothest PDMS surface (Figure 2a) because of higher level of cross-linking density. The water contact angle measurement revealed that the PDMS surface became more hydrophobic by increasing the base to cross-linker ratio (Figure 2f), which could be due to two important effects. First, the hydrophobic methyl groups in the prepolymer increases with the base proportion thus reducing the surface wettability.[42,43] Second, the increased surface nanoroughness can further reduce the wettability due to formation of air pockets between the nanoridges.[44,45] In addition, the surface stiffness has been suggested to be more relevant to cell−substrate interactions compared to bulk elastic modulus of the substrate material.[46] Therefore, we used AFM indentation method to measure the compressive modulus of the treated PDMS surface. It was observed that the PDMS surface stiffness decreased from 70.44 ± 9.166 to 13.8 ± 2.315 kPa when increasing the polymer base proportion, which was corresponding to a lower level of cross-linking (Figure 2g).

The initial cell adhesion and proliferation is usually an indicator of the surface biocompatibility, which depends on the chemical composition at the cell−substrate interface such as the type and density of surface ligands,[47,48] and also on the physical properties such as roughness, stiffness and hydrophobicity of the substrate.[49−51] Therefore, we first characterized the initial cell adhesion immediately after cell seeding and also monitored the cell proliferation continuously for 7 days. Initially, variation of the combinatorial PDMS surface properties showed no significant short-term effect on cell adhesion (Figure 3a) or proliferation (Figure 3b) at day 1, although the coated fibronectin exhibited much higher concentration on 5:1 PDMS compared to other substrates (Figure S2, Supporting Information). However, the long-term effect of PDMS substrate properties on hBMSC proliferation became more obvious starting from Day 3 (Figure 3b), which showed that the proliferation rate was enhanced considerably on the PDMS substrates with the highest level of cross-linking (base/curing agent = 5:1). The statistical significance for Day 3 data was $^{**}p < 0.0001$, which was lower than those for days 5 and 7 data ($^{*}p < 0.05$). This observed reduction of statistical significance was due to the increased standard deviations (error bars) for each data group at later stages of culture because the inevitable human errors during initial cell seeding (e.g., errors in seeding density or volume) were magnified when the cells continued to grow. On the other hand, the difference between the mean values for 5:1 PDMS compared to other PDMS groups increased obviously in the prolonged culture, although their statistical significance was reduced. These results indicated that the PDMS formulation influenced long-term hBMSC proliferation although it did not affect the initial cell adhesion and proliferation. It further suggested that the combinatorial effect of higher stiffness, lower hydrophobicity and lower roughness of the PDMS substrate enhanced hBMSC proliferation. These observations were consistent with prior studies on the individual effects of multiple surface properties, which reported that stiffer,[25,52] smoother,[53] or less hydrophobic[54] surfaces could promote the proliferation of multiple types of stem cells.

The spreading and migration of hBMSCs on fibronectin-coated PDMS substrates was shown in Figure 4. It was

DOI: 10.1021/acsami.5b03753
ACS Appl. Mater. Interfaces 2015, 7, 17095−17103

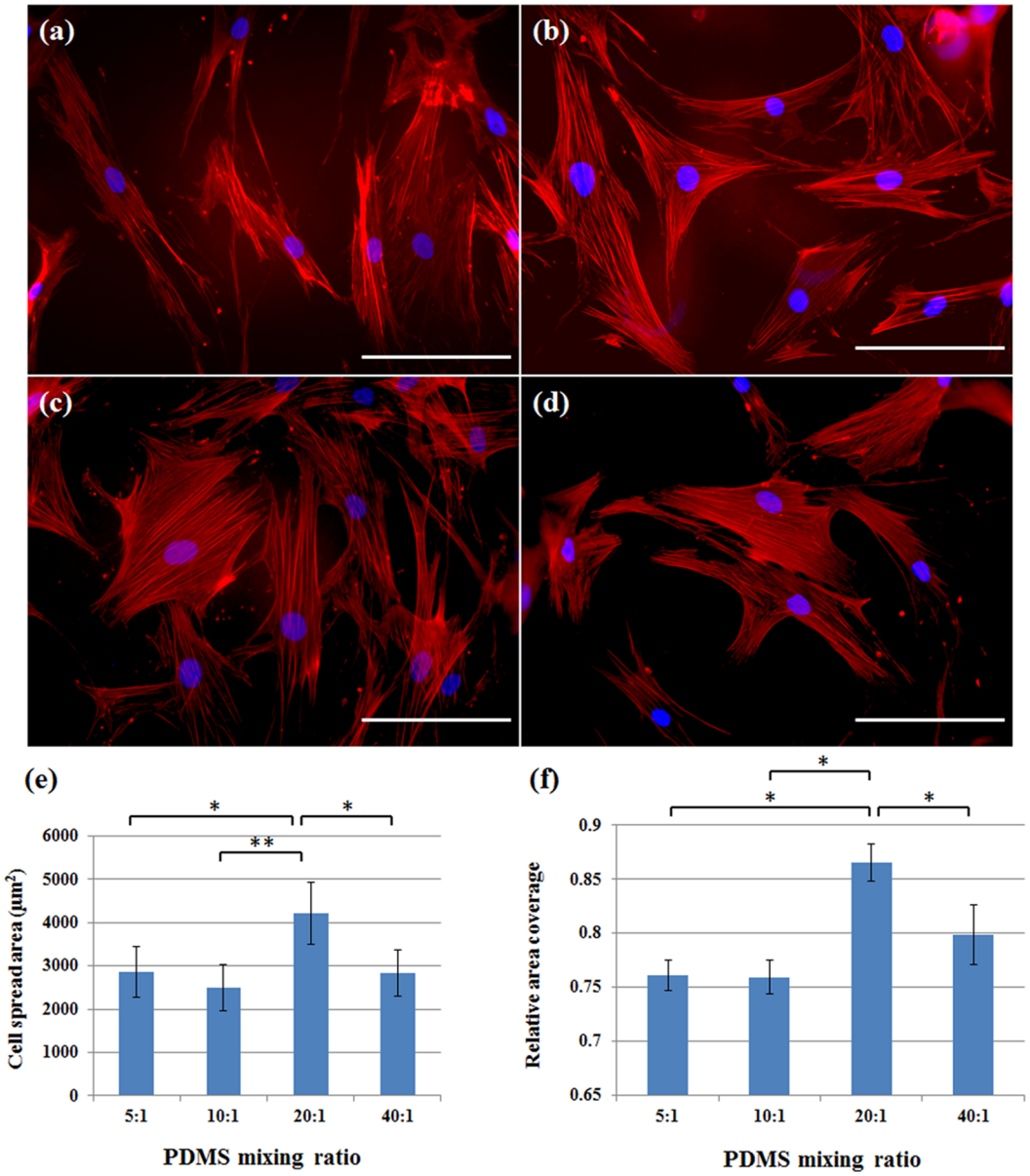

Figure 4. Fluorescence staining for F-actin (red) and nucleus (blue) of the cell culture on different PDMS substrates at day 7: (a) 5:1, (b) 10:1, (c) 20:1, and (d) 40:1. Scale bars: 50 μm. (e) Individual cell spreading area. (f) The total area covered by the migrating cells with respect to the total area of the central compartment. $^{**}p < 0.0001$, $^{*}p < 0.05$, $n = 5$.

observed that most cells exhibited a typical spindle-like shape, while more cells appeared with wider spreading area and rounded shape on the PDMS substrates formulated with lower proportion of cross-linker (Figure 4a–d). The quantitative measurements (Figure 4e) by mapping the contour of individual cells further revealed that the cell spreading was optimum on the 20:1 PDMS substrate, which was featured by roughness (4.37 ± 0.72 nm) and stiffness (21.76 ± 3.22 kPa) at intermediate level among all the samples tested while remaining slightly hydrophobic (contact angle = 105.08° ± 3.21°).

Consistent with individual cell spreading, the total area covered by the migrating cell population also reached maximum on the 20:1 PDMS substrate at day 7 (Figure 4f). Compared to many wound healing assays (e.g., scratch assay or physical barrier assay) that induce fast wound closure, the 7-day cell migration assay in this study took much longer time due to some inherent differences. In a regular wound healing assay, there is an injury that is usually inflicted on a cell sheet either by a mechanical scratch (scratch assay) or through removal of a physical barrier (on the cells growing along the edge of the barrier). These wounds stimulate the release of growth factors that can promote fast closure of the wound. In the present study, there was no such injury caused and we did not use any chemokines for stimulation of expedited cell migration. This was the major reason that the cell migration took much longer time for about 6 days, excluding the initial day for cell attachment and proliferation. In addition, it has been reported that hBMSCs (passage 6) have a doubling time of about 72 h.[55] Some prior works have further shown that the wound healing assay of approximately 500 μm in width (comparable to the central channel in this study) can take twice of the time cost for the cells to double their quantity.[56] Therefore, the time cost for the hBMSC migration in our study was consistent with those findings in the literature. Furthermore, the corresponding total

DOI: 10.1021/acsami.5b03753
ACS Appl. Mater. Interfaces 2015, 7, 17095–17103

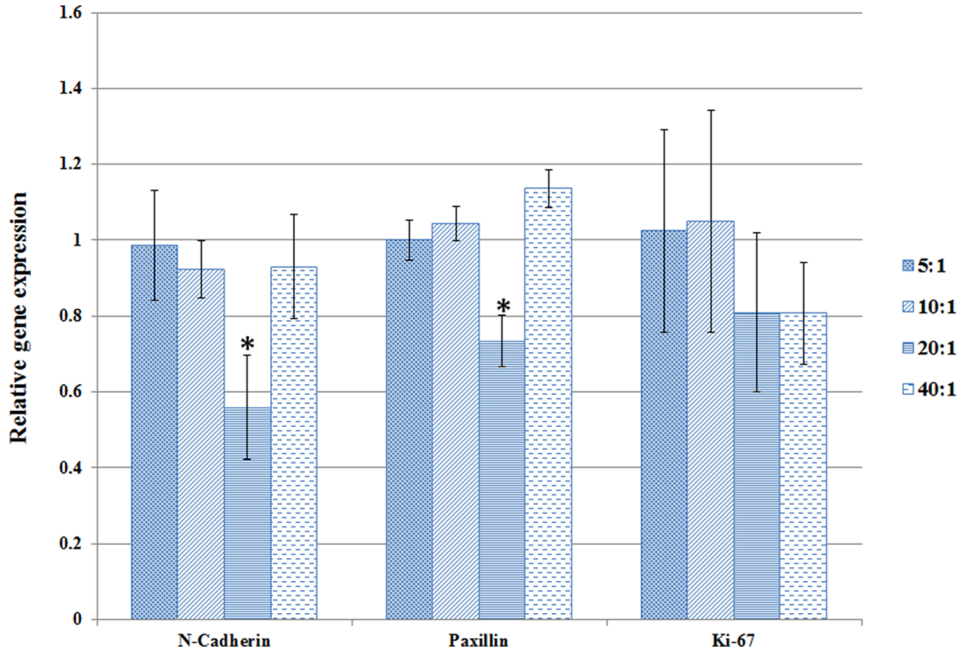

Figure 5. Real time PCR assays of the hBMSCs at day 5 cultured on different PDMS substrates. All data were normalized with regard to the gene expression on 5:1 PDMS. *$p < 0.05$, $n = 3$.

number count of the migrating cells by nucleus DAPI staining (Figure S3, Supporting Information) exhibited the same trend as compared with the measured spreading area in Figure 4e–f. On the other hand, the total area coverage of the migrating cells was expected to be much higher considering the multiplication effect (single cell spreading area × number counts). However, the dense cell distribution on 20:1 PDMS led to a higher level of cell overlap (Figure 4c). When the contour mapping software computed the total cell coverage, it could not differentiate the overlapping cells and thus could not take these overlapped area into account. Therefore, the total cell coverage as shown in Figure 4f was underestimated due to cell overlap. In the literature, many previous studies showed that changes of a single aspect of surface properties could have either promotional or inhibitory effect on cell migration. For example, it was reported that stiffer,[51,57] roughened,[58,59] or more hydrophilic[54,60] surfaces usually enhanced cell spreading. However, the variations of PDMS cross-link levels led to profound changes in many important aspects of surface properties simultaneously, including stiffness, roughness, and hydrophobicity (Figure 2), which had a combinatorial effect on cell migration (Figure 4) that was different from those caused by the changes of any individual aspect of surface properties. As discussed above, the hBMSC spreading and migration were most favored on 20:1 PDMS substrate, which exhibited intermediate levels of roughness, stiffness and hydrophobicity.

To understand the observed change of cell migration on different substrates at a molecular level, quantitative real time PCR (qRT PCR) assay was performed to examine the gene expression of typical adhesion protein markers that were associated with cell migration behavior, including paxillin (cell–substrate linkage) and N-cadherin (cell–cell junction). Paxillin downregulation was shown to be associated with decreased cell migration of hBMSCs.[61] N-cadherin downregulation was associated with increased cell migration in human hematopoietic progenitor cells and smooth muscle cells,[62,63] while N-cadherin upregulation was associated with cell condensation thus leading to reduced migration of hBMSC.[64,65] Figure 5 indicated that the expression of paxillin and N-cadherin in the hBMSCs on 20:1 PDMS substrates was substantially lower than those on other substrates made with different mixing ratios, while the cell spreading and migration reached optimum on 20:1 PDMS (Figure 4). These results were consistent with a previous report that paxillin down-regulation caused a decrease in N-cadherin expression thus resulting in enhanced migration of Hela cells.[66] Furthermore, the gene expression of proliferation marker Ki-67 (Figure 5) revealed slightly higher proliferation rate on the substrates with lower base proportions (5:1 and 10:1), which was consistent with the results by cell proliferation assay (Figure 3b). The proliferation assay and gene analysis further suggested that the cell coverage in the central channel on 20:1 PDMS was mainly due to cell migration from the side channels rather than cell proliferation.

CONCLUSIONS

This study has demonstrated an efficient way to study the combinatorial impact of substratum properties on cell behavior using a microfluidic migration assay. The physical properties of PDMS, including hydrophobicity, surface roughness and stiffness, can be easily tuned by varying the prepolymer to curing agent ratio. It was observed that although the initial cell adhesion and proliferation were similar on all PDMS substrates, cell spreading and migration appeared to be most favored on 20:1 PDMS that exhibited an intermediate level of roughness, stiffness and hydrophobicity. These findings indicated that multiple aspects of surface properties had a combinatorial impact on cell behavior, which was different from the effects caused by the changes of any individual aspect of surface properties. Since cell migration is a vital process during tissue generation, this study may elucidate important physical cues desirable in the development of scaffolds with enhanced cell migration potential for stem cell based regenerative medicine.

DOI: 10.1021/acsami.5b03753
ACS Appl. Mater. Interfaces 2015, 7, 17095–17103

■ ASSOCIATED CONTENT

Supporting Information

More figures and tables for cell migration, number counts, surface bound proteins, and PCR assays. The Supporting Information is available free of charge on the ACS Publications website at DOI: 10.1021/acsami.5b03753.

■ AUTHOR INFORMATION

Corresponding Author

*E-mail: yuejun.kang@ntu.edu.sg. Phone: +65 6790 4702. Fax: +65 6794 7553.

Author Contributions

N.V.M., Y.J.C., and Y.K. conceived the experiments, N.V.M. and S.P. designed and conducted the microfluidic experiments, Y. Z. and V.C. conducted the AFM experiments, N.V.M. and Y.J.C. conducted the substrate compatibility tests, N.V.M., Y.J.C., and Y.W. analyzed the results, N.V.M. and Y.K. wrote the manuscript. All the authors reviewed and approved the manuscript.

Notes

The authors declare no competing financial interest.

■ ACKNOWLEDGMENTS

Y.K. acknowledges the funding support by a Tier 2 Academic Research Fund (ARC 22/13) and a Tier 1 Academic Research Fund (RG 37/14) from the Ministry of Education of Singapore. The Ph.D. scholarship from Nanyang Technological University awarded to N.V.M. is gratefully acknowledged.

■ REFERENCES

(1) Arthur, A.; Zannettino, A.; Gronthos, S. The Therapeutic Applications of Multipotential Mesenchymal/Stromal Stem Cells in Skeletal Tissue Repair. *J. Cell. Physiol.* **2009**, *218*, 237−245.

(2) Barry, F. P.; Murphy, J. M. Mesenchymal Stem Cells: Clinical Applications and Biological Characterization. *Int. J. Biochem. Cell Biol.* **2004**, *36*, 568−584.

(3) Sundelacruz, S.; Kaplan, D. L. Stem Cell- and Scaffold-Based Tissue Engineering Approaches to Osteochondral Regenerative Medicine. *Semin. Cell Dev. Biol.* **2009**, *20*, 646−655.

(4) Barbash, I. M.; Chouraqui, P.; Baron, J.; Feinberg, M. S.; Etzion, S.; Tessone, A.; Miller, L.; Guetta, E.; Zipori, D.; Kedes, L. H.; Kloner, R. A.; Leor, J. Systemic Delivery of Bone Marrow−Derived Mesenchymal Stem Cells to the Infarcted Myocardium: Feasibility, Cell Migration, and Body Distribution. *Circulation* **2003**, *108*, 863−868.

(5) Drury, J. L.; Mooney, D. J. Hydrogels for Tissue Engineering: Scaffold Design Variables and Applications. *Biomaterials* **2003**, *24*, 4337−4351.

(6) Kim, D.-H.; Provenzano, P. P.; Smith, C. L.; Levchenko, A. Matrix Nanotopography as a Regulator of Cell Function. *J. Cell Biol.* **2012**, *197*, 351−360.

(7) Kleinman, H. K.; Philp, D.; Hoffman, M. P. Role of the Extracellular Matrix in Morphogenesis. *Curr. Opin. Biotechnol.* **2003**, *14*, 526−532.

(8) Watt, F. M. The Extracellular Matrix and Cell Shape. *Trends Biochem. Sci.* **1986**, *11*, 482−485.

(9) Reig, G.; Pulgar, E.; Concha, M. L. Cell Migration: From Tissue Culture to Embryos. *Development* **2014**, *141*, 1999−2013.

(10) Li, S.; Guan, J.-L.; Chien, S. Biochemstry and Biomechanics of Cell Motility. *Annu. Rev. Biomed. Eng.* **2005**, *7*, 105−150.

(11) Brandl, F.; Sommer, F.; Goepferich, A. Rational Design of Hydrogels for Tissue Engineering: Impact of Physical Factors on Cell Behavior. *Biomaterials* **2007**, *28*, 134−146.

(12) Han, J.; Menon, N. V.; Kang, Y.; Tee, S.-Y. An in Vitro Study on the Collective Tumor Cell Migration on Nanoroughened Poly-(Dimethylsiloxane) Surfaces. *J. Mater. Chem. B* **2015**, *3*, 1565−1572.

(13) Shin, H. Fabrication Methods of an Engineered Microenvironment for Analysis of Cell−Biomaterial Interactions. *Biomaterials* **2007**, *28*, 126−133.

(14) Zhu, J.; Marchant, R. E. Design Properties of Hydrogel Tissue-Engineering Scaffolds. *Expert Rev. Med. Devices* **2011**, *8*, 607−626.

(15) Bose, S.; Roy, M.; Bandyopadhyay, A. Recent Advances in Bone Tissue Engineering Scaffolds. *Trends Biotechnol.* **2012**, *30*, 546−554.

(16) Mace, K. A.; Hansen, S. L.; Myers, C.; Young, D. M.; Boudreau, N. Hoxa3 Induces Cell Migration in Endothelial and Epithelial Cells Promoting Angiogenesis and Wound Repair. *J. Cell Sci.* **2005**, *118*, 2567−2577.

(17) Chen, H. C. Boyden Chamber Assay. *Methods Mol. Biol.* **2005**, *294*, 15−22.

(18) Meyvantsson, I.; Beebe, D. J. Cell Culture Models in Microfluidic Systems. Annu. *Annu. Rev. Anal. Chem.* **2008**, *1*, 423−449.

(19) Voldman, J.; Gray, M. L.; Schmidt, M. A. Microfabrication in Biology and Medicine. *Annu. Rev. Biomed. Eng.* **1999**, *1*, 401−425.

(20) Beebe, D. J.; Mensing, G. A.; Walker, G. M. Physics and Applications of Microfluidics in Biology. *Annu. Rev. Biomed. Eng.* **2002**, *4*, 261−286.

(21) Cimetta, E.; Cannizzaro, C.; James, R.; Biechele, T.; Moon, R. T.; Elvassore, N.; Vunjak-Novakovic, G. Microfluidic Device Generating Stable Concentration Gradients for Long Term Cell Culture: Application to Wnt3a Regulation of [Small Beta]-Catenin Signaling. *Lab Chip* **2010**, *10*, 3277−3283.

(22) Chung, S.; Sudo, R.; Mack, P. J.; Wan, C.-R.; Vickerman, V.; Kamm, R. D. Cell Migration into Scaffolds under Co-Culture Conditions in a Microfluidic Platform. *Lab Chip* **2009**, *9*, 269−275.

(23) Sia, S. K.; Whitesides, G. M. Microfluidic Devices Fabricated in Poly(Dimethylsiloxane) for Biological Studies. *Electrophoresis* **2003**, *24*, 3563−3576.

(24) Leclerc, E.; Sakai, Y.; Fujii, T. Cell Culture in 3-Dimensional Microfluidic Structure of Pdms (Polydimethylsiloxane). *Biomed. Microdevices* **2003**, *5*, 109−114.

(25) Eroshenko, N.; Ramachandran, R.; Yadavalli, V. K.; Rao, R. R. Effect of Substrate Stiffness on Early Human Embryonic Stem Cell Differentiation. *J. Biol. Eng.* **2013**, *7*, 7.

(26) Palchesko, R. N.; Zhang, L.; Sun, Y.; Feinberg, A. W. Development of Polydimethylsiloxane Substrates with Tunable Elastic Modulus to Study Cell Mechanobiology in Muscle and Nerve. *PLoS One* **2012**, *7*, e51499.

(27) Park, J.; Yoo, S.; Lee, E.-J.; Lee, D.; Kim, J.; Lee, S.-H. Increased Poly(Dimethylsiloxane) Stiffness Improves Viability and Morphology of Mouse Fibroblast Cells. *BioChip J.* **2010**, *4*, 230−236.

(28) Shen, Y.; Wang, G.; Huang, X.; Zhang, Q.; Wu, J.; Tang, C.; Yu, Q.; Liu, X. Surface Wettability of Plasma Sio(X):H Nanocoating-Induced Endothelial Cells' Migration and the Associated Fak-Rho GTPases Signalling Pathways. *J. R. Soc., Interface* **2012**, *9*, 313−327.

(29) Lo, C. M.; Wang, H. B.; Dembo, M.; Wang, Y. L. Cell Movement Is Guided by the Rigidity of the Substrate. *Biophys. J.* **2000**, *79*, 144−152.

(30) Pelham, R. J.; Wang, Y.-l. Cell Locomotion and Focal Adhesions Are Regulated by Substrate Flexibility. *Proc. Natl. Acad. Sci. U. S. A.* **1997**, *94*, 13661−13665.

(31) DiMilla, P. A.; Stone, J. A.; Quinn, J. A.; Albelda, S. M.; Lauffenburger, D. A. Maximal Migration of Human Smooth Muscle Cells on Fibronectin and Type IV Collagen Occurs at an Intermediate Attachment Strength. *J. Cell Biol.* **1993**, *122*, 729−737.

(32) Hansen, T. D.; Koepsel, J. T.; Le, N. N.; Nguyen, E. H.; Zorn, S.; Parlato, M.; Loveland, S. G.; Schwartz, M. P.; Murphy, W. L. Biomaterial Arrays with Defined Adhesion Ligand Densities and Matrix Stiffness Identify Distinct Phenotypes for Tumorigenic and Non-Tumorigenic Human Mesenchymal Cell Types. *Biomater. Sci.* **2014**, *2*, 745−756.

DOI: 10.1021/acsami.5b03753
ACS Appl. Mater. Interfaces 2015, 7, 17095−17103

(33) Peyton, S. R.; Putnam, A. J. Extracellular Matrix Rigidity Governs Smooth Muscle Cell Motility in a Biphasic Fashion. *J. Cell. Physiol.* **2005**, *204*, 198−209.
(34) Stroka, K. M.; Aranda-Espinoza, H. Neutrophils Display Biphasic Relationship between Migration and Substrate Stiffness. *Cell Motil. Cytoskeleton* **2009**, *66*, 328−341.
(35) Mih, J. D.; Marinkovic, A.; Liu, F.; Sharif, A. S.; Tschumperlin, D. J. Matrix Stiffness Reverses the Effect of Actomyosin Tension on Cell Proliferation. *J. Cell Sci.* **2012**, *125*, 5974−5983.
(36) Trkov, S.; Eng, G.; Di Liddo, R.; Parnigotto, P. P.; Vunjak-Novakovic, G. Micropatterned Three-Dimensional Hydrogel System to Study Human Endothelial−Mesenchymal Stem Cell Interactions. *J. Tissue Eng. Regener. Med.* **2010**, *4*, 205−215.
(37) McDonald, J. C.; Duffy, D. C.; Anderson, J. R.; Chiu, D. T.; Wu, H.; Schueller, O. J.; Whitesides, G. M. Fabrication of Microfluidic Systems in Poly(Dimethylsiloxane). *Electrophoresis* **2000**, *21*, 27−40.
(38) Menon, N. V.; Chuah, Y. J.; Cao, B.; Lim, M.; Kang, Y. A Microfluidic Co-Culture System to Monitor Tumor-Stromal Interactions on a Chip. *Biomicrofluidics* **2014**, *8*, 064118.
(39) Wu, Y.-N.; Law, J. B. K.; He, A. Y.; Low, H. Y.; Hui, J. H. P.; Lim, C. T.; Yang, Z.; Lee, E. H. Substrate Topography Determines the Fate of Chondrogenesis from Human Mesenchymal Stem Cells Resulting in Specific Cartilage Phenotype Formation. *Nanomedicine* **2014**, *10*, 1507−1516.
(40) Li, D.; Ding, J.; Wang, X.; Wang, C.; Wu, T. Fibronectin Promotes Tyrosine Phosphorylation of Paxillin and Cell Invasiveness in the Gastric Cancer Cell Line Ags. *Tumori* **2009**, *95*, 769−779.
(41) Rago, L.; Beattie, R.; Taylor, V.; Winter, J. Mir379−410 Cluster Mirnas Regulate Neurogenesis and Neuronal Migration by Fine-Tuning N-Cadherin. *EMBO J.* **2014**, *33*, 906−920.
(42) Fuard, D.; Tzvetkova-Chevolleau, T.; Decossas, S.; Tracqui, P.; Schiavone, P. Optimization of Poly-Di-Methyl-Siloxane (PDMS) Substrates for Studying Cellular Adhesion and Motility. *Microelectron. Eng.* **2008**, *85*, 1289−1293.
(43) Michael, J. O., Siloxane Surface Activity. *In Silicon-Based Polymer Science*; American Chemical Society: Washington, DC, 1989; Chapter 40, pp 705−739.
(44) Borgioli, F.; Galvanetto, E.; Bacci, T. Influence of Surface Morphology and Roughness on Water Wetting Properties of Low Temperature Nitrided Austenitic Stainless Steels. *Mater. Charact.* **2014**, *95*, 278−284.
(45) Yoshimitsu, Z.; Nakajima, A.; Watanabe, T.; Hashimoto, K. Effects of Surface Structure on the Hydrophobicity and Sliding Behavior of Water Droplets. *Langmuir* **2002**, *18*, 5818−5822.
(46) Seo, J.-H.; Sakai, K.; Yui, N. Adsorption State of Fibronectin on Poly(Dimethylsiloxane) Surfaces with Varied Stiffness Can Dominate Adhesion Density of Fibroblasts. *Acta Biomater.* **2013**, *9*, 5493−5501.
(47) Chastain, S. R.; Kundu, A. K.; Dhar, S.; Calvert, J. W.; Putnam, A. J. Adhesion of Mesenchymal Stem Cells to Polymer Scaffolds Occurs Via Distinct Ecm Ligands and Controls Their Osteogenic Differentiation. *J. Biomed. Mater. Res., Part A* **2006**, *78A*, 73−85.
(48) Lee, J. W.; Kim, Y. H.; Park, K. D.; Jee, K. S.; Shin, J. W.; Hahn, S. B. Importance of Integrin B1-Mediated Cell Adhesion on Biodegradable Polymers under Serum Depletion in Mesenchymal Stem Cells and Chondrocytes. *Biomaterials* **2004**, *25*, 1901−1909.
(49) Ayala, R.; Zhang, C.; Yang, D.; Hwang, Y.; Aung, A.; Shroff, S. S.; Arce, F. T.; Lal, R.; Arya, G.; Varghese, S. Engineering the Cell−Material Interface for Controlling Stem Cell Adhesion, Migration, and Differentiation. *Biomaterials* **2011**, *32*, 3700−3711.
(50) Gail, M. H.; Boone, C. W. Cell-Substrate Adhesivity: A Determinant of Cell Motility. *Exp. Cell Res.* **1972**, *70*, 33−40.
(51) Li, J.; Han, D.; Zhao, Y.-P. Kinetic Behaviour of the Cells Touching Substrate: The Interfacial Stiffness Guides Cell Spreading. *Sci. Rep.* **2014**, *4*, 1−10.
(52) Rowlands, A. S.; George, P. A.; Cooper-White, J. J. Directing Osteogenic and Myogenic Differentiation of Mscs: Interplay of Stiffness and Adhesive Ligand Presentation. *Am. J. Physiol.: Cell Physiol* **2008**, *295*, C1037−1044.
(53) Kawahara, H.; Soeda, Y.; Niwa, K.; Takahashi, M.; Kawahara, D.; Araki, N. In Vitro Study on Bone Formation and Surface Topography from the Standpoint of Biomechanics. *J. Mater. Sci.: Mater. Med.* **2004**, *15*, 1297−1307.
(54) Hao, L.; Yang, H.; Du, C.; Fu, X.; Zhao, N.; Xu, S.; Cui, F.; Mao, C.; Wang, Y. Directing the Fate of Human and Mouse Mesenchymal Stem Cells by Hydroxyl-Methyl Mixed Self-Assembled Monolayers with Varying Wettability. *J. Mater. Chem. B* **2014**, *2*, 4794−4801.
(55) Kern, S.; Eichler, H.; Stoeve, J.; Klüter, H.; Bieback, K. Comparative Analysis of Mesenchymal Stem Cells from Bone Marrow, Umbilical Cord Blood, or Adipose Tissue. *Stem Cells* **2006**, *24*, 1294−1301.
(56) Kim, H. N.; Hong, Y.; Kim, M. S.; Kim, S. M.; Suh, K.-Y. Effect of Orientation and Density of Nanotopography in Dermal Wound Healing. *Biomaterials* **2012**, *33*, 8782−8792.
(57) Yeung, T.; Georges, P. C.; Flanagan, L. A.; Marg, B.; Ortiz, M.; Funaki, M.; Zahir, N.; Ming, W.; Weaver, V.; Janmey, P. A. Effects of Substrate Stiffness on Cell Morphology, Cytoskeletal Structure, and Adhesion. *Cell Motil. Cytoskeleton* **2005**, *60*, 24−34.
(58) Lampin, M.; Warocquier-Clérout, R.; Legris, C.; Degrange, M.; Sigot-Luizard, M. F. Correlation between Substratum Roughness and Wettability, Cell Adhesion, and Cell Migration. *J. Biomed. Mater. Res.* **1997**, *36*, 99−108.
(59) Lipski, A. M.; Pino, C. J.; Haselton, F. R.; Chen, I. W.; Shastri, V. P. The Effect of Silica Nanoparticle-Modified Surfaces on Cell Morphology, Cytoskeletal Organization and Function. *Biomaterials* **2008**, *29*, 3836−3846.
(60) Kuddannaya, S.; Chuah, Y. J.; Lee, M. H. A.; Menon, N. V.; Kang, Y.; Zhang, Y. Surface Chemical Modification of Poly-(Dimethylsiloxane) for the Enhanced Adhesion and Proliferation of Mesenchymal Stem Cells. *ACS Appl. Mater. Interfaces* **2013**, *5*, 9777−9784.
(61) Yun, S. P.; Ryu, J. M.; Han, H. J. Involvement of Beta1-Integrin Via Pip Complex and Fak/Paxillin in Dexamethasone-Induced Human Mesenchymal Stem Cells Migration. *J. Cell. Physiol.* **2011**, *226*, 683−692.
(62) Wein, F.; Pietsch, L.; Saffrich, R.; Wuchter, P.; Walenda, T.; Bork, S.; Horn, P.; Diehlmann, A.; Eckstein, V.; Ho, A. D.; Wagner, W. N-Cadherin Is Expressed on Human Hematopoietic Progenitor Cells and Mediates Interaction with Human Mesenchymal Stromal Cells. *Stem Cell Res.* **2010**, *4*, 129−139.
(63) Blindt, R.; Bosserhoff, A.-K.; Dammers, J.; Krott, N.; Demircan, L.; Hoffmann, R.; Hanrath, P.; Weber, C.; Vogt, F. Downregulation of N-Cadherin in the Neointima Stimulates Migration of Smooth Muscle Cells by Rhoa Deactivation. *Cardiovasc. Res.* **2004**, *62*, 212−222.
(64) DeLise, A. M.; Tuan, R. S. Alterations in the Spatiotemporal Expression Pattern and Function of N-Cadherin Inhibit Cellular Condensation and Chondrogenesis of Limb Mesenchymal Cells in Vitro. *J. Cell. Biochem.* **2002**, *87*, 342−59.
(65) Gao, L.; McBeath, R.; Chen, C. S. Stem Cell Shape Regulates a Chondrogenic Versus Myogenic Fate through Rac1 and N-Cadherin. *Stem Cells* **2010**, *28*, 564−572.
(66) Yano, H.; Mazaki, Y.; Kurokawa, K.; Hanks, S. K.; Matsuda, M.; Sabe, H. Roles Played by a Subset of Integrin Signaling Molecules in Cadherin-Based Cell−Cell Adhesion. *J. Cell Biol.* **2004**, *166*, 283−295.

DOI: 10.1021/acsami.5b03753
ACS Appl. Mater. Interfaces 2015, 7, 17095−17103